2014 IEEE XXXIV International Scientific Conference Electronics and Nanotechnology (ELNANO)

Contact Properties of Ultrasmall Carbon Nanotube Transistors from *Ab-initio*

Artem Fediai, Dmytry Ryndyk, Gianaurelio Cuniberti
Institute for Materials Science and Max Bergmann Center of Biomaterials
Center for Advancing Electronics Dresden
Dresden Center for Computational Materials Science
TU Dresden
Dresden, Germany
artem.fediai@nano.tu-dresden.de

***Abstract* — based on large-scale *ab-initio* calculations contact properties of carbon nanotubes field effect transistors with 9-nm channel were analyzed. We have found that the internal part of the nanotube is metalized, while the uncovered CNT portion is p-doped due to the influence of the metal. Our findings can explain unique scaling of the CNT-FETs based on first-principles.**

Keywords — carbon nanotube transistor; ab-initio; contact

I. INTRODUCTION

Carbon nanotubes (CNT) are one of the most promising candidates as channels for next generation field-effect transistors (FET) due unique electronic properties and recent advances in CNT-FET technology [1]. CNT-FETs have high current densities, linear transconductance characteristic, low subthreshold swing close to theoretical limit of 60 mV/dec [2]; recently it has been shown that ultrasmall (down to 9 nm) CNTFETs show unique performance [3], which is even better than those were theoretically predicted before.

Like in any electronic component, the reduction of the contact resistance is of critical importance in CNT-FETs. In conventional electronics, the semiconductor near the contact with the metallic electrode is degenerately doped to avoid Schottky barrier appearing. According to our knowledge, creation of a good contact without doping of semiconductor has never been achieved in practice. It would seem that apparent approach to develop low-ohmic CNT-metal contacts would be a doping of the CNT near the contact. CNT doping, however, is a challenging task that has not been resolved yet [4]. This is due to the nature of CNT, which is a surface object itself and has no bulk.

Nevertheless, back in 2003 IBM has shown experimentally that Pd electrodes are able to provide ohmic contact for holes for CNTs with diameter larger than ~1.7 nm without doping [5]. Later on, also ohmic contacts for electrons were fabricated by using scandium [6], yttrium [7], gadolinium [8], erbium and lanthanum [9]. Until now there is no rigorous explanation, why contacts with the mentioned metals are ohmic while another are Schottky-type one.

There are methods allowing determination Schottky barrier height from the density functional theory (DFT). Those are potential profile line-up method [10] and its extension, which taking contact dipole into account [11, 12, 13]. Both these methods came from Tung's work [14], who considered planar contacts only, and, strictly speaking, cannot be applied as is to the contact with complicated shape, but they were. If the citing works would consider sufficiently thick tubes (with diameter larger than 1.3 nm), for which there are many experimental data, one could verify these methods. Although, only small-diameter CNTs (chirality (8,0), (10,0)) were simulated, for which barrier with Pd were found from the value as small as 0.03 eV [13] till the value as large as 0.4 eV [12].

Unlike conventional planar contacts, even deeply embedded into the metal portion of CNT plays important role in overall resistance of a contact, and should be taken into account. One of the most prominent evidence of distributed nature of the contact between metal and CNT is experimentally observed strong dependence of the contact resistance on the depth of CNT embedding [15] up to the contact length as large as 300 nm. Earlier in [16] it was predicted that this could have place for distributed contacts in principle if interaction between metal and CNT is weak sufficiently; but it has been done only in qualitative level.

Until now, no sound explanation of the unique scaling of CNT-FET [3] was given by ab-initio methods. There is a work [17], which tries it, but it uses end-contact instead of embedded contact, and Al instead of Pd, which makes its conclusions questionable.

In this work we consider the most realistic geometry compared to those were used until now. First, we have taken nanotube with the diameter and the length resembles realistic CNTFETs; second we have embedded it into sufficiently deep and sufficiently thick slab of a metal. This transition to large-scale DFT allows us to explain unique scaling behavior of CNT-FETs based on the first-principle calculations. The results are quite unexpected and can be obtained only by performing large-scale *ab-initio* calculations.

II. CONTACT GEOMETRIES TO BE SIMULATED

In theoretical works commonly considering type of CNT-metal contacts are "end-contacts" and "side contacts". We consider in this work another type of the contact, when long portion of the CNT is embedded into the metal. It is the type

978-1-4799-4580-1/14/$31.00 ©2014 IEEE

that being used in modern CNT-FETs due to its low resistance.

Embedded contacts differ from semiconductor-metal contacts in conventional electronics. In the embedded contact electrons/holes enter CNT along relatively long embedded portion of the CNT.

Such "distributed" nature of electron transport means that there are two sources that limit current flow from metal to CNT. They are (1) external contact, which is between embedded and free-standing CNT and (2) internal contact which is the border between CNT embedded into the metal and the latter. Notable, external contact has a cylindrical shape (2-D), and external contact is a circle (1-D). This has crucial importance, when trying to apply methods, developed for planar contacts.

Our system of consideration was developed as a compromise between experimental set-up, described in [3] and available computational resources needed to perform *ab-initio* calculation.

In [3] relevant part of the smallest CNTFET consists of 20-nm long electrodes, and the channel itself is a 9-nm long CNT. Available numerical resources are far not sufficient to simulate ab-initio the whole transistor. Therefore, we have partition the system into the two subsystems, which represent both types of the contacts.

To understand internal contact we consider the cell comprising 2 periods of CNT (17-0) embedded into 3 periods of Pd (011) slab (hereafter "Structure 1", denoted at fig. 1 as a "supercell"). Minimum distance between C and Pd atoms is kept to be less than 2.1 Å. Cross-section area of the Pd slab is 27,23x27,5 $Å^2$.

For external contact we consider 22 periods of a free CNT attached by both ends to 2 supercells, used for internal contact and described above (hereafter called "Structure 2"), fig 1.

Geometry of the contacts and the channel is in a good agreement with those of the CNT-FET developed by IBM in the work [3] (see Table I).

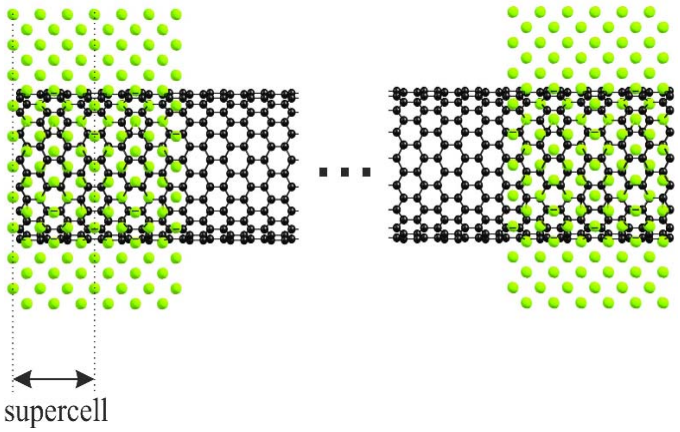

Fig. 1. Longitudinal view of the CNT-FET channel, embedded into the Pd

TABLE I. GEOMERY PARAMETERS

Parameter	**This work**	**Franklin *et. al.* [3]**
Diameter of CNT	1.39 nm	(1.3±0.2) nm
chirality	(17-0)	n. a.
Length of a channel	9,36 nm	9 nm
Electrode's metal	Pd	Pd
Orientation a metallic slab	(011)	n. a.
Contact length	3,3 nm	20 nm

III. GENERAL THEORETICAL FRAMEWORK

In order to obtain ground state of the many-particle system set by geometry pointed out above we use density functional theory as implemented in the module "Quickstep" of CP2K Package [18]. DFT allows substituting initial N-electron quantum-mechanical problem by the problem of one single particle moving in effective potential. The distinctive feature of DFT realization in cp2k is using hybrid Gaussian and plane wave basis (GPW) [19], which provide necessary acceleration for as large system as we have in hand. In GPW method there are two representations for electron density $\rho(\mathbf{r})$:

1) In terms of contracted Gaussian functions: $\rho(\mathbf{r}) = \sum_{\mu,\nu} P^{\mu\nu}\varphi_\mu(\mathbf{r})\varphi_\nu(\mathbf{r})$ with $\varphi_i = \sum_j d_{ji} g_j(\mathbf{r})$, where $g_j(\mathbf{r})$ are primitive Gaussian functions, d_{ji} are contraction coefficients.

2) In terms of plane waves: $\tilde{\rho}(\mathbf{r}) = \frac{1}{\Omega}\sum_{\mathbf{G}} \tilde{\rho}(\mathbf{G})\exp(i\mathbf{G}\mathbf{r})$, where $\mathbf{G}$ is reciprocal wave vector.

As φ_i we have used optimized SZV basis set for C atoms and DZVP basis set for Pd atoms as discussed in [20]. The energy functional $E(\rho)$ consists of the contributions, as follow:

$$E[\rho] = E^T[\rho] + E^V[\rho] + E^H[\rho] + E^{XC}[\rho] + E^{II}, \qquad (1)$$

where E^T is electronic kinetic energy; E^V is the energy of electron-ionic cores interaction, E^H is the Hartree energy, E^{XC} is exchange-correlation energy; E^{II} is the energy of interionic interaction. Terms 1, 2 and 4 in (1) are expressed in Gaussian plane-wave basis, whereas Hartree energy is expressed in the plane-wave basis.

Electron-cores interaction $E^V[\rho]$ in (1) is splitting into the local and nonlocal part. The first one is taking into account by using pseudopotentials of Goedecker, Teter and Hutter [21, 22]. As an approximation of exchange-correlation potential we use meta-generalized gradient approximation (GGA) of Perdue, Burke and Ernzerhof (PBE) [23].

IV. QUANTITIES EXTRACTED FROM DFT CALCULATIONS

We are focusing on the two physical quantities to analyze qualitatively CNT-metal contact: difference electron density and local density of states, projected onto carbon's orbitals.

A. *Projected Density of States Analysis*

As a result of DFT calculations we obtain number of energy levels corresponding to Kohn-Sham Hamiltonian. Total density of states is formally defined as:

$$g(E) = \sum_i \langle \psi_i | \psi_i \rangle \delta(E - E_i), \quad (2)$$

where E_i and ψ_i are eigenenergies and eigenvectors of the Kohn-Sham Hamiltonian; $\langle \psi_i | \psi_i \rangle = 1$.

Density of states, projected onto j-th orbital (PDOS) of orthogonal basis $\{|\chi_j\rangle\}$ is defined, combining identity

$$I = \sum_j |\chi_j\rangle\langle\chi_j|, \quad (3)$$

and (2) yielding:

$$g_j(E) = \sum_i \langle \psi_i | \psi_i \rangle \delta(E - E_i) \equiv \sum_i \langle \psi_i | \sum_j |\chi_j\rangle\langle\chi_j| |\psi_i\rangle \delta(E - E_i) = \sum_j |\langle \psi_i | \chi_j \rangle|^2 \delta(E - E_i), \quad (4)$$

The quantity $|\langle \psi_i | \chi_j \rangle|^2$ appeared in (4) is called PDOS.

As the basis of contracted Gaussian functions used in cp2k is nonorthogonal and (3) is no more valid, the basis is first orthogonalizing as described in [24], and only then (4) is used. We have projected DOS onto all orthogonalized carbon orbitals of a SZV basis set, i.e. $2s$, $2p_x$, $2p_y$, $2p_z$.

Although it is not possible within cp2k to get spatially resolved (local) projected density of states (LDOS), we have evaded this problem by giving carbon atoms belonging different supercells different names and then projecting total DOS onto the orbitals of these atoms.

The system in hand is finite, thus all above defined DOSes are superposition of δ -like function. The latter can be defined, for instance, by limiting procedure:

$$\delta(E) \equiv \frac{1}{\pi} \lim_{\Gamma \to 0} \frac{\Gamma/2}{(E - E_i)^2 + (\Gamma/2)^2} \quad (5)$$

For better visualization we use instead of limiting procedure (5) small, but finite Γ to define $\delta(E)$ in (2). This will also reflect the fact that the system, attached to electrodes have continuous spectrum of states. For the forthcoming plots we use $\Gamma = 8\,\text{meV}$.

The distribution of the density of states, projected onto carbon atoms along the tube is shown at fig. 2. The central part of the nanotube remains semiconductor-like, but Fermi level is shifted down to the valence band edge (see also fig. 3). One can say that nanotube is p-doped far from the contacts. Embedded portion of the nanotube, indeed, behave itself like a metal or heavily doped p-type semiconductor, as there are many states near the Fermi level there (see also fig. 3). There is a transition region between the metallized contacts and p-doped semiconducting channel. In order to express the distribution of the density of states in terms of the band diagram commonly used in electronics we have defined valence Ev and conduction Ec band edges as follows: $N_0 = \int_{E_{ref}}^{E_c} g(E,x)dE$, $N_0 = \int_{E_v}^{E_{ref}} g(E,x)dE$, where N0 – is some not too large number of states (we have chosen $N = N_0/200$, where $N \equiv \int_{-1\,\text{eV}}^{1\,\text{eV}} g(E, x=0)dx$); $E_{ref} = 0.2\,\text{eV}$ is a reference level. Thus, we have defined band gap as an energy range containing only 1% of the states within the region [-1 eV; 1 eV].

B. *Charge Transfer within Internal Contact*

In order to estimate charge transfer between carbon nanotube deeply embedded into the metal and the metal itself we have defined average surface difference charge density in the Structure 1 (fig. 4) as follows:

$$\Delta\rho_S(x,y) = \frac{1}{L_z}\int_0^{Lz} \{\rho_{all}(\mathbf{r}) - \rho_C(\mathbf{r}) - \rho_{Pd}(\mathbf{r})\}\,dz,$$

where ρ_{all}, ρ_C, ρ_{Pd} are electron density distribution in the Structure 1, and in the same structure containing only carbon and palladium atoms, respectively.

Charge redistribution reveals that the charge income will take place between carbon and palladium atoms. In turns, electrons outcome take place from the π-orbitals of the carbon atoms; σ-orbitals gain more electrons. To estimate charge transfer rate between C and Pd atoms we have applied Bader analysis [25], as implemented in [26]. It has shown that each carbon atom donates $5.5\cdot10^{-3}$ electrons, whereas each Pd atom accept $3.5\cdot10^{-3}$ electrons in average.

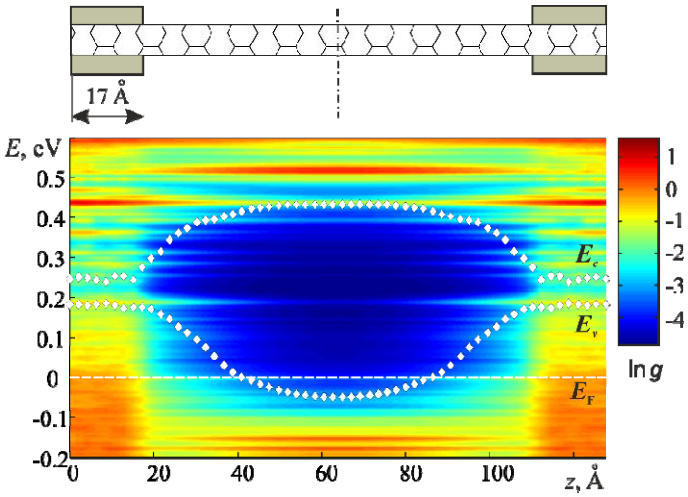

Fig. 2. Projected density of states $g(E)$ onto carbon atoms along nanotube

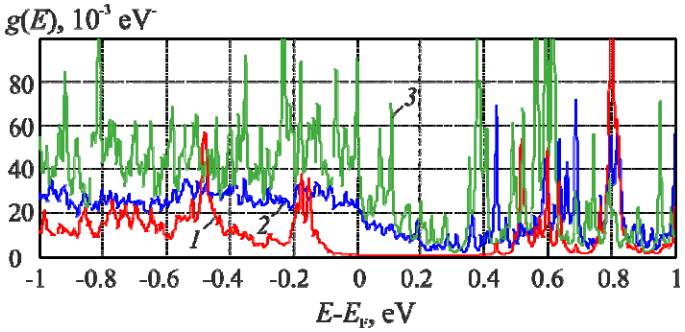

Fig. 3. Local density of states of the unit cell of CNT: at the center of the System 2 (*1*) ; at the embedded part of the CNT in System 2 (*2*); in the System 1 (*3*)

C. Charge Transfer within External Contact

In order to define charge redistribution near the external CNT-metal contact we have simulated the whole *Structure* 2; then divided it into the two parts and simulated them separately. The first part is embedded CNT and the metal covered it; the second part is a portion of CNT free from the metal.

In order to evaluate charge transfer between the electrode with embedded nanotube and free nanotube we have averaged difference charge density to define average electron density income in z-direction:

$$\Delta\rho_l(z) = \frac{1}{L_x L_y}\int_0^{Lx}\int_0^{Ly}\left\{\rho_{all}(\mathbf{r}) - \rho_{emb}(\mathbf{r}) - \rho_{free}(\mathbf{r})\right\} dx\, dy\,,$$

where ρ_{all}, ρ_{emb}, ρ_{free} are electron density in the Structure 2, in the first and second subsystem of the System 1, accordingly.

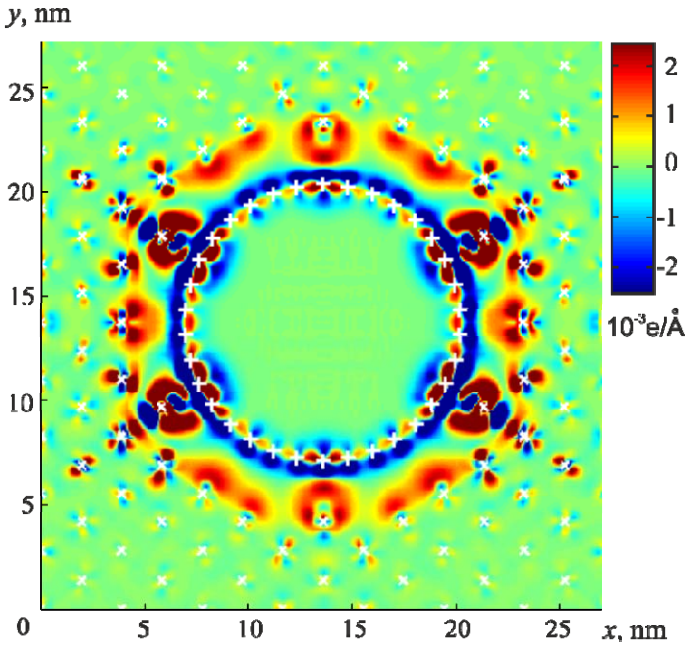

Fig. 4. Average surface charge density in the embedded nanotube (transverse direction). Positions of the Pd and C atoms is denote by symbols "x" and "+", respectively

Distribution $\Delta\rho_l(z)$ is almost symmetric with respect to the border of external contact (fig. 5). This indicates that conductance in both direction from external contact is almost constant. Such behavior agrees with the distribution of partial LDOS on carbon atoms along the CNT (fig. 5), which shows CNT metallization inside the metal and smooth transition to the *p*-doped type away from the contact. Such kind of the contact is reminiscent the contact between metal and degenerately *doped* semiconductor, although we have a contact between the metal and *intrinsic* semiconductor. Therefore, it is not necessary to perform doping of CNT to avoid external contact: doping takes place naturally.

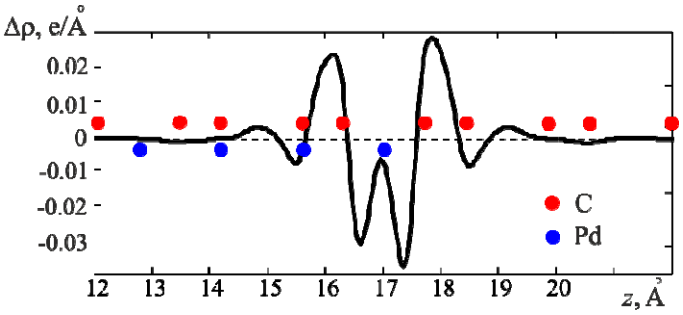

Fig. 5. Charge density difference near the external contact (averaged over transverse direction)

V. Conclusion

We have performed large-scale DFT simulation of the contacts and the channel of CNT-FET closely resembles CNT-FET with 9-nm channel from [3]. Based on the analysis of the spatially resolved density of states, projected onto carbon atoms and charge transfer analysis, we conclude that Pd atom causes metallization of the embedded CNT's portion and natural p-type doping of the uncovered CNT's portion.

We have used longitudinal distribution of the local density of states in order to define conduction and valence band edges, which can be used in simplified electrical models.

In conventional metal-oxide-semiconductor FETs in order to get rid of the contact barrier, semiconductor near the contact with the electrodes is doped degenerately; in the case of CNT-FET with Pd electrodes, metal-induced p-type doping near the contact take place naturally. In the present case of 9-nm channel, we observe also the doping of the whole nanotube as a result of ultrashort channel length. It is expected to disappear for the CNT-FETs with longer channels.

To our knowledge, the system we have simulated is the largest CNT-metal system that have ever been simulated by DFT. This has given us an access to the information about the actual CNT-metal contact properties in real CNT-FET contacts at the *ab-initio* level.

Acknowledgment

We acknowledge the Center for Information Services and High Performance Computing (ZIH) at TU Dresden for computational resources. This work is partly supported by the

German Research Foundation (DFG) within the Cluster of Excellence "Center for Advancing Electronics Dresden".

REFERENCES

[1] A. D. Franklin, «Electronics: The road to carbon nanotube transistors,» *Nature*, vol. 498, pp. 443-444, 2013.

[2] A. D. Franklin, N. A. Bojarczuk and M. Kopel, «Consistently low subthreshold swing in carbon nanotube transistors using lanthanum oxide,» *Appl. Phys. Lett.*, vol. 102, p. 013108, 2013.

[3] A. D. Franklin, *et.al.*, «Sub-10 nm Carbon Nanotube Transistor,» *Nano Letters*, vol. 12(2), pp. 758-762, 2012.

[4] M. Schroter, M. Claus, P. Sakalas, M. Haferlach and D. Wang, «Carbon Nanotube FET Technology for Radio-Frequency Electronics: State-of-the-Art Overview,» *IEEE Journal of the Electron Devices Society*, vol. 1(1), pp. 9-20, 2013.

[5] A. Javey, Q. W. Jing Guo, M. Lundstorm and H. Dai, «Ballistic carbon nanotube field-effect transistors,» *Nature*, vol. 424, pp. 654-657, 2003.

[6] L. Ding, *et.al.*, «Y-Contacted High-Performance n-Type Single-Walled Carbon Nanotube Field-Effect Transistors: Scaling and Comparison with Sc-Contacted Devices,» *Nano Letters*, vol. 12, pp. 4209-4214, 2009.

[7] Z. Zhang, *et.al*., «Doping-Free Fabrication of Carbon Nanotube Based Ballistic CMOS Devices and Circuits,» *Nano Letters*, vol. 7(12), pp. 3603-3607, 2007.

[8] C. Wang, K. Ryu, A. Badmaev, J. Zhang and C. Zhou, «Metal Contact Engineering and Registration-Free Fabrication of Complementary Metal-Oxide Semiconductor Integrated Circuits Using Aligned Carbon Nanotubes,» *ACS Nano*, vol. 5 (2), pp. 1147-1153, 2011.

[9] D. Shahrjerdi, A. D. Franklin, S. Oida, J. A. Ott, G. S. Tulevski and W. Haensch, "High-Performance Air-Stable n-Type Carbon Nanotube Transistors with Erbium Contacts," *ACS Nano*, № 7(9), pp. 8303-8308, 2013.

[10] B. Shan and K. Cho, "First Principles Study of Work Functions of Single Wall Carbon Nanotubes," *Phys. Rev. Lett*., vol. 94, p. 236602, 2005.

[11] Y. He, J. Zhang, M. Zhang, Y. Wang and Z. Yu, "Chemical Bonding and Schottky Barrier for Metal-Carbon Nanotube Contacts," *13th International Workshop on Computational Electronics*, IWCE, 2009.

[12] Y. He, J. Zhang, S. Hou, Y. Wang and Z. Yu, "Schottky barrier formation at metal electrodes and semiconducting carbon nanotubes," *Appl. Phys. Lett*., vol. 94, p. 093107, 2009.

[13] V. Vitale, A. Curioni and W. Andreoni, "Metal-Carbon Nanotube Contacts: The Link between Schottky Barrier and Chemical Bonding," *Journal of the American Chemical Society*, vol 130(13), pp. 5848-5849, 2008.

[14] R. T. Tung, "Formation of an electric dipole at metal-semiconductor interfaces," *Phys. Rev. B*, vol. 64, p. 205310, 2001.

[15] A. D. Franklin and Z. Chen, "Length scaling of carbon nanotube transistors," *Nature Nanotechnology*, vol. 5, pp. 858-862, 2010.

[16] D. Tomanek and N. Nemec, "Modeling extended contacts for nanotube and graphene devices," *Phys. Rev. B*, vol. 77 (12), p. 125420, 2008.

[17] Y.-H. Kim and H. S. Kim, "Anomalous length scaling of carbon nanotube-metal contact resistance: An ab-initio study," *Appl. Phys. Lett.*, vol. 100, p. 213113, 2012.

[18] J. VandeVondele, M. Krack, F. Mohamed, M. Parrinello, T. Chassaing and J. Hutter, «Quickstep: Fast and accurate density functional calculations using a mixed Gaussian and plane waves approach,» *Computer Physics Communications*, vol. 167(2), pp. 103 - 128, 2005.

[19] G. Lippert, J. Hutter and M. Parrinello, «A hybrid Gaussian and plane wave density functional scheme,» *Molecular Physics*, vol. 92 (3), pp. 477-488, 1997.

[20] J. VandeVondele and J. Hutter, "Gaussian basis sets for accurate calculations on molecular systems in gas and condensed phases," *J. Chem. Phys*., vol. 127, p. 114105, 2007.

[21] S. Goedecker, M. Teter and J. Hutter, "Separable dual-space Gaussian pseudopotentials," *Phys. Rev. B*., vol. 54, p. 1703, 1996.

[22] C. Hartwigsen, S. Goedecker and J. Hutter, "Relativistic separable dual-space Gaussian pseudopotentials from H to Rn," *Phys. Rev. B*, vol. 58, p. 3641, 1998.

[23] J. P. Perdew, K. Burke and M. Ernzerhof, "Generalized Gradient Approximation Made Simple," *Phys. Rev. Lett*., vol. 77 (18), pp. 3865-3868, 1996.

[24] P.-O. Löwdin, "On the Non-Orthogonality Problem Connected with the Use of Atomic Wave Functions in the Theory of Molecules and Crystals," *J. Chem. Phys*., vol. 18, pp. 365-375 , 1949.

[25] R. Bader, Atoms in molecules: A Quantum Theory, New York: Oxford University Press, 1990.

[26] W. Tang, E. Sanville and G. Henkelman, «A grid-based Bader analysis algorithm without lattice bias,» *Journal of Physics: Condensed Matter*, vol. 21, p. 084204, 2009.